Mapping Diseased Oak Trees Using ADAR Imagery

Maggi Kelly and **Desheng Liu**
Center for the Assessment and Monitoring of Forest and Environmental Resources
Ecosystem Sciences Division
Department of Environmental Science, Policy and Management
University of California at Berkeley
151 Hilgard Hall, #3110. Berkeley, CA 94720-3110, USA.
E-mail: mkelly@nature.bekeley.edu
dliu@nature.berkeley.edu

Abstract

We investigated the ability of high spatial-resolution 4-band imagery (Airborne Digital Acquisition and Registration - ADAR) to discern moisture stress in trees affected by Sudden Oak Death (SOD). We wanted to test if the imagery could be used to distinguish between green oak trees with advanced SOD trunk symptoms, and green oaks with no SOD trunk symptoms. ADAR imagery of China Camp State Park in Marin County, California was flown in spring 2000 and 2001. Training samples from the field consisting of the locations green healthy oaks and green symptomatic oaks were used to derive spectral signatures for the two classes. Both hierarchical unsupervised classification (HUC) and maximum likelihood classification (MLC) were used to classify the imagery. Accuracy assessment and other spectral measurements were performed to analyze the separability of the two signatures. Poor overall accuracy 55.17% was obtained by the HUC method. A better overall accuracy 74.19% was obtained by MLC method, but the low transformed divergence (1448) indicated poor separability of the training samples. The poor accuracy results can be explained by the fact that ADAR image has relatively broad spectral bands that combine narrow moisture- stress-sensitive regions with broader stress-insensitive regions; such combination could decrease the capability of ADAR to detect moisture stress. In addition, healthy oaks in the area display a marked variability in canopy condition, making it difficult to separate healthy trees from those experiencing some stress. In conclusion, this research indicated the inability to automate mapping of moisture stress in oaks using ADAR imagery, and limited success in using methods that require extensive field data.

Introduction

The epidemic currently killing tens of thousands of coast live oaks (*Quercus agrifolia*), black oaks (*Quercus kelloggii*) and tanoaks (*Lithocarpus densiflorus*) in California is referred to as sudden oak death (SOD) (Rizzo *et al*. 2002). The disease can kill several species of trees and shrubs, and California redwood (*Sequoia sempervirens*) has recently been confirmed as a host. The causal pathogen *Phytophthora ramorum* has been officially confirmed on hosts in 12 coastal counties of California, and hosts for the disease exist in several more counties throughout the state (Figure 1). The disease has reached epidemic proportions in some areas (Rizzo *et al*. 2002) with infection levels over 50% (McPherson *et al*. 2002). SOD has received substantial attention by the media and the pubic because oaks not only represent a major component of many California hardwood forest ecosystems, they are also important both in urban landscapes and at the urban/rural interface (Garbelotto *et al*. 2001).

The disease progression on individual trees is relatively well understood (Garbelotto *et al*. 2001; Rizzo *et al*. 2002). There are two forms of the disease: in the foliar type the pathogen colonizes the leaves of hosts, and in the main stem form of the disease *P. ramorum* enters the main stem of the plant. It is with this latter form of the disease that we are concerned here, as it is accompanied by dramatic crown symptoms. After the pathogen infects the main stem of a susceptible tree, cankers develop in the phloem tissue and can extend to the xylem (Rizzo *et al*. 2002). These cankers exude a darkish red substance (termed here and in the press "bleeding") on the main stem. They grow rapidly, and over time can girdle the tree, effectively disrupting moisture and nutrient movement in the tissue. Rapid (2 - 4 weeks) crown fading and color change follows in many cases, and this is usually preceded by extensive cankering (Rizzo *et al*. 2002). While early symptomology (canker existence) has not been associated with leaf moisture stress (Swiecki and Bernhardt 2002), we are assuming that trees with advanced stem symptoms (extensive cankers and bleeding) and within one year of changing color are experiencing leaf moisture stress.

The disease displays clustering at landscape scales (Kelly and Meentemeyer 2002), with clumps of dead and dying trees clearly visible from above. The condition and spatial pattern of oaks with the disease can be crucial indicators of

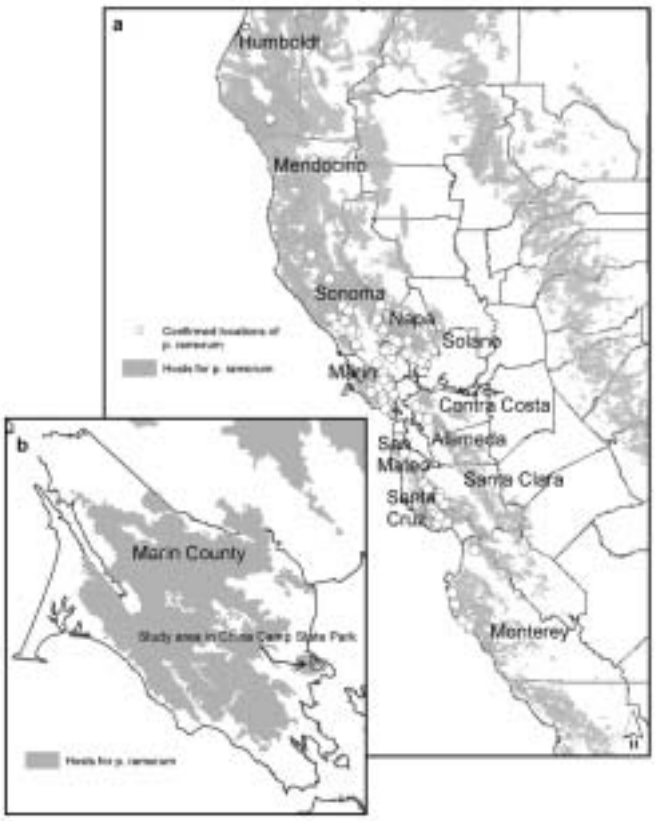

Figure 1 The study area in China Camp State Park in Marin County, California: a) locations of confirmed cases of p. ramorum in California as of October 2002, and distribution of hosts for the disease, and b) Marin County, showing the location of China Camp State Park.

disease progression. Patterns of spatial variation of the syndrome's progression through a stand can serve as a key diagnostic tool, illuminating possible mechanisms of transmission among trees and interactions among casual agents (Kelly and McPherson 2001). In addition, the trees affected by the disease are potential fire sources because the water content of leaves is largely lost due to girdling of the tree stem by advanced canker development (Rizzo *et al*. 2002). Because of these factors, the ability to use remotely sensed data to discern trees undergoing moisture stress as a result of the disease before their canopy changes color (a condition we call "previsual stress") would be a valuable scientific aid and management tool.

Remote sensing of vegetation stress

The use of remote sensing for mapping vegetation stress relies on knowledge regarding the relationship between the chemical and physical structure, the moisture content of leaves and incoming light (Ceccato *et al*. 2001; Cibula *et al*. 1992; Curran 1989; Elvidge 1990; Jensen 2000). Chlorophyll and moisture content of leaves are key factors in the remote sensing of vegetation stress. The structure of the leaf, and the spectral features of water dominate green leaf reflectance in the near infrared portions of the spectrum, and chlorophyll presence and water dominate reflectance in the visible ranges (Cibula *et al*. 1992; Curran 1989; Elvidge 1990). Vegetation stress can be manifested as a loss of leaf water content, or as a decrease in chlorophyll content. Reflectance in stressed leaves changes dramatically in the visible range (including increases in the chlorophyll absorption bands and fluorescence) and in the NIR ranges due to these losses and to the consequent revelation of leaf chemical composites that were masked by water in the healthy leaf (Elvidge 1990; Jensen 2000).

Most traditional sensors (e.g. the "broader wave range and fewer classes" approach (vanAardt and Wynne 2001)) are designed to capture reflected light in broad ranges sensitive to vegetation characteristics (i.e. ~ 450nm, 500nm and 650nm for visible light, and ~800nm for NIR reflectance). These data with broad spectral ranges and broad spatial coverage have been employed in a variety of vegetation applications, including crop monitoring, drought and fire damage in conifer forests and recent examples of studies pertaining to heath of hardwood forests (Cohen 1991; Duchemin *et al*. 1999; Everitt *et al*. 1999; Macomber and Woodcock 1994; Pinder and McLeod 1999). Cibula *et al*. (1992) described the possibility of using Thematic Mapper (TM) bands for vegetation stress monitoring, and concluded that while bands 5 and 7 are extremely useful for detection of moisture content, band 4 also correlated well with a decrease in leaf water content. Macomber and Woodcock (1994) used TM imagery to map conifer mortality as a result of drought, and point out the utility of traditional remote sensors (broad coverage, low spectral resolution) for forest hazard management by providing both locations and estimates of tree mortality. Pinder and McLeod (1999) also used TM imagery to examine vegetation moisture content and found some correlation (although small: $r^2 = 0.16 - 0.36$) between a band 5/4 ratio and historic rainfall (using tree ring data). Duchemin *et al.* (1999) found that NDVI derived from NOAA-AVHRR imagery was useful in determining water status of forests over a broad area, although Cohen (1994) found an inconsistent relationship between TM NDVI and water content.

New possibilities for remote sensing of vegetation and stress detection were made possible with the advent of hyperspectral imaging (vanAardt and Wynne 2001). Recent work investigating vegetation stress and remote sensing utilizes hyperspectral data both at the leaf scale using spectrometers and at the canopy scale using hyperspectral imaging tools. Gong *et al*. (1997) used a field spectrometer to successfully differentiate between six confer species. Pu *et al*. (in press) showed that water moisture content in coast live oak leaves was correlated with absorption features across the spectrum, but particularly at 975 nm, 1200 nm and 1750 nm. While one of their initial goals was to differentiate between healthy and stressed trees, they were unable to do so in that study. Tian *et al*. (2001) obtained high prediction accuracy between spectral absorption features between 1650 and 1850 nm and relative water content (RWC) of wheat. At the canopy scale, Ustin *et al*. (1998) found that AVIRIS data of moderate spatial resolution (20-m) was promising for developing regional estimates of canopy water content for chaparral shrubs. Green vegetation fluorescence has also

been used as an indicator of stress as it relates directly to the amount of chlorophyll in a leaf (Flexas *et al*. 2000). Zarco-Tejada *et al*. (2000) found a link between hardwood canopy and chlorophyll fluorescence in the 680 - 690 nm range at the leaf scale as well as the canopy scale using CASI data (Zarco-Tejada *et al*. 2000).

This review demonstrates that great success has been found in detecting vegetation moisture stress using hyperspectral imagery; however, there have been successes in deriving water stress from coarser spectral resolution data. Our work here mimics that of the TM studies mentioned above but with higher spatial resolution; we use 1-m ADAR imagery with four bands that emulate TM bands 1-4. And while the automatic discrimination of oak trees with moisture stress from course spectral resolution data is a challenging task, there are obvious and pressing management justifications for attempting to do so. Moreover, the pathology of this new disease affords an opportunity for development of techniques for remote sensing in hardwood forests in general, and stressed hardwood forests in particular because it has a dramatic overstory component that takes place quickly. Researchers working on the SOD project have used ADAR 4-band imagery to map dead oaks (Kelly and Meentemeyer 2002; Kelly 2002) with good accuracy (90-95%). Specifically, this research evaluates the feasibility of distinguishing the spectral signatures of green oak trees with advanced SOD symptoms on the main stem (thus assumed to be undergoing some degree of moisture stress) and green oaks with no SOD symptoms on the main stem. The results are valuable to further research in mapping the disease through time, and for determining the spatial pattern and moisture-stress component of the disease progression.

Methods

Study Site

The study site for this project is a forested peninsula on the east side of Marin County (Figure 1) called China Camp State Park. The area has moderate to steep topography, with elevations ranging from sea level at San Pablo Bay (the northerly lobe of the San Francisco Bay) to over 300m. The forest stands there are near even-age stands; these hillsides were cleared for lumber in the early to mid-1800s. The forest canopy here is largely continuous; individual trees have moderately large canopies (from 4m2-16m2). Coast live, black and valley oaks are abundant, and occur in mixed stands with mature madrone and bay trees providing habitat to a variety of wildlife, including deer, squirrels and numerous birds. All of these trees with the exception of valley oak are hosts for Phytophthora ramorum (Rizzo *et al*. 2002). The disease was first noticed in the area in 1997, and the disease was widespread through the forest in 2000 (Kelly 2002; McPherson *et al*. 2002).

Data Description

High-resolution Imagery. Imagery used in this project consisted of ADAR 5500 (Airborne Data Acquisition and Registration) imagery acquired for the China Camp study area in spring 2000 and 2001. The ADAR 5500 imaging system is comprised of a 20mm lens with four mounted cameras (spectral bands: band1 (blue): 450-550nm, band 2 (green): 520-610nm, band 3 (red): 610-700nm, band 4 (near infrared): 780-920nm), flown at an average aircraft altitude of 2,205m. The cameras have a large field of view (typically about 35 degrees from nadir) and so collect high spatial-resolution data from relatively low altitudes with large aerial coverage. The average ground spatial resolution of our imagery is 1-meter. Imagery was acquired and georeferenced by a private contractor (Positive Systems Inc. of Montana). Individual frames were color-balanced prior to mosaicing by correcting for internal lens effects (vignetting), sun angle artifacts and exposure differences by the contractor. No atmospheric correction was applied to the mosaiced imagery; the image was flown at low altitude, there were no difference in atmosphere across the study area, and there was no visible reason to correct for atmospheric effects. Georeferencing used a nearest neighbor resampling method, achieving 0.5m RMSE.

Field data. We gathered training samples for use in the supervised classification and for accuracy assessment of both the supervised and unsupervised methods. Training samples and accuracy assessment samples for the spectral signature creation and evaluation were gathered in the field in summer 2001. The location of 25 healthy coast live oak trees with medium to large crowns (>3m diameter), green foliage, and no SOD symptoms on the tree trunk were located with GPS, and on hardcopy printouts of the 2001 and 2002 imagery. Each crown was clearly distinguishable on the imagery. The location of 28 stressed coast live oaks with medium to large green crowns were found by first locating individual trees in the imagery that were dead in the 2001 imagery but appeared healthy in the imagery from 2000, and then locating those individuals in the field with GPS and on hardcopy imagery printout (Figure 2). These stressed trees had advanced symptoms on the main stem (extensive cankering and bleeding) and were within one year of changing color from green to brown. Ten of the healthy samples and thirteen of the stressed samples were reserved for accuracy assessment.

Spectral classes. The locations of the samples were then transferred from the hardcopy printout to the screen, making sure the center of each target crown was digitized as a point. The pixel neighborhood surrounding each point was used as a training sample for signature development in the supervised classification process. The size of this sample window changed according to the crown closure of trees, from 3x3 to 7x7 in the case of the largest crowns.

Classification

Both unsupervised classification and supervised classification were used to determine the spectral separability of the two samples. We employed a hierarchical method for the unsupervised approach.

Hierarchical Unsupervised Classification (HUC). We

broke the study area into five general land cover types: water, wetland, road, bare ground, and hardwood forest. We made three assumptions about the spectral variability in the study area so that we could concentrate our research on the hardwood forest. First, due to the spectral similarity between bare land and dead or dying oaks, we did not classify the dead or dying trees as part of the hardwood forest, but included them in the bare ground category. We did this to reduce the size of the targeted spectral data; we were not interested in dead trees, only stressed trees, and dead trees are very similar in spectral properties to bare soil. Second, we grouped other vegetation in the area (non-oak species, dense forbs or shrubs) with the hardwood forest class in the first level of the hierarchical scheme. Third, we assumed that the forest canopy is dominated by oak trees.

In order to improve the computation efficiency and classification accuracy, we utilized a hierarchical unsupervised classification to extract stressed oaks from the image in two steps. The hierarchical strategy avoids the influence of the inter-variance of non-target classes on the differentiation within target classes (Lobo *et al*. 1997; Townsend and Walsh 2001). In our case, since the inter-variance of non-target classes is much bigger than that within the target class, the clustering algorithm splits the classes with bigger inter-variance into several sub-classes while keeping the stressed oaks and healthy oaks as the same tree class in the first level of the classification hierarchy.

First, the image was clustered into five general land cover classes (water, wetland, road, bare ground, and hardwood forest); the stressed oaks and healthy oaks were clustered in the same general class. Second, the non-tree class was masked out and the resulting image was further clustered into two subclasses: stressed oaks and healthy oaks. The ISODATA clustering algorithm was used to cluster the spectrally similar pixels into two classes using the four bands. This resulted in each tree being divided into two classes (see Figure 3a). We also constrained the algorithm to find three and four classes. Here we wanted to remove the influence of shadows by forcing shadow pixels into a separate class (or classes). This resulted in more visible striping effect on individual tree crowns (Figure 3). We visually determined that the two class run best approximated individual trees and the results from the ISODATA clustering with two classes using four bands was evaluated for accuracy.

Supervised Classification. We used a NDVI (Normalized Difference Vegetation Index) to separate vegetation (all the trees and part of the vegetated bare land) from the other non-vegetation features in the original image. NDVI is a useful enhancement in pre-classification analysis because it is sensitive to vegetation greenness, and it is least affected by topographic changes (Lyon *et al*. 1998). An optimal threshold

Figure 2 ADAR imagery (false color transformation (4,3,2)) of the study area. Ground control points are superimposed on the imagery.

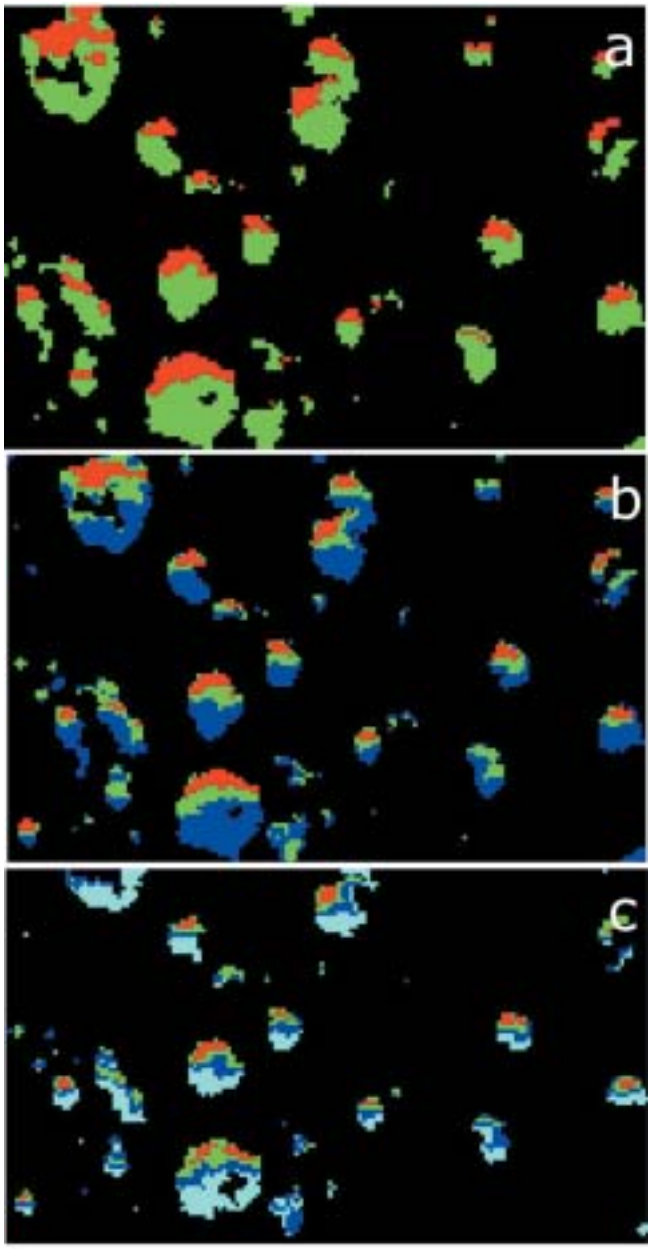

Figure 3 Example of striping within tree crowns resulting from unsupervised classification. Classification results with a) two classes, b) three classes, and c) four classes.

(NDVI = -0.012) was selected to mask out all the non-vegetation by observing the peak and tail from the NDVI histogram.

Once the non-vegetation class was removed, shadows of trees remained and were treated as a separate class in order to reduce the effect of shadow on the differentiation between stressed oaks and healthy oaks. The training samples (the 3x3, 5x5 or 7x7 pixel cluster representing each target crown, and samples of tree shadows digitized from the screen) were used to develop spectral signatures using Erdas Imagine Signature Editor (Erdas 1999). After signature creation, the signature separability between the two oak classes was evaluated using a transformed divergence measurement and viewed in a feature space plot. A transformed divergence value of above 1900 provides good separability while below 1700 is poor (Jensen 2000). A maximum likelihood classifier was performed to classify the preprocessed image into three classes (healthy, stressed and shadow) using the signature with the best separability measure.

Accuracy Assessment

An accuracy assessment was performed for each of the classifications (supervised and unsupervised) based on the ground truth data reserved for this purpose. Producer's accuracy (probability of a reference pixel being correctly classified, or omission error), user's accuracy (probability that a pixel classified on the final product represents that category on the ground, or commission error), overall accuracy, and a Kappa coefficient were calculated for each classification algorithm. The Kappa coefficient is commonly recommended as a suitable accuracy measure in thematic classification because it helps to determine whether the results are significantly better than a random result (Khat = 0) (Jensen 1996). Since the goals of this method were not to map different spectral classes, no error matrix was generated.

Results

Hierarchical Unsupervised Classification

The original image was clustered into five general land cover types: forest, bare land, road, wetland, and water. The forest class was further classed into three classes (healthy and stressed oaks, and shadows) using the ISODATA classifier. The results showed a clear striping within each tree: the number of stripes corresponded to the number of classes found (Figure 3). This suggests that the spectral variation within an individual tree (including the tree shadow) was larger than the variation between the healthy and stressed individuals.

Supervised Classification

The histograms for the digital numbers (for four bands) of all training pixels are shown in Figure 4. There is considerable overlap between the two classes, predicting a poor classification result. Spectral separability between healthy oaks and stressed oaks was calculated by a transformed divergence (Table 1). All separability measures listed here are below the generally accepted minimum standard for the transformed divergence measure of 1700 (Jensen 2000). The best separability (1448) was obtained with the combination of band three and band four.

Feature space plots provide great insight into the information content of the image and the degree of between-band correlation. We plotted the signatures of the stressed oaks and healthy oaks from band four versus all visible bands (Figure 5). These ellipses, centered on the mean vector, describes the main distribution of the signature in the feature space. In all three images clear overlap between the two signatures can been seen. In all cases the variability of healthy oaks is large, and the ellipse defining the spectral signature of healthy oaks subsumes most of the spectral variability of the target stressed oaks. Despite this, we used the maximum likelihood classification algorithm to classify the preprocessed image using band 3 and band 4 into three information classes: stressed oaks, healthy oaks, and shadows.

Accuracy Assessment

We performed an accuracy assessment for each of the classifications using the ground truth data reserved for this purpose. Producer's accuracy, user's accuracy, overall accuracy, and Kappa coefficient were calculated to assess the classification accuracy. The accuracy matrices for the supervised (MLC) and unsupervised (ISODATA) classifiers are shown in Table 2. The unsupervised classification method

Table 1 Signature separability measures (transformed divergence) between healthy and stressed oaks derived for ADAR bands.

Band number	Best Band Combination	Transformed Divergence
1	2	1132
2	3, 4	1448
3	2, 3, 4	1096
4	1, 2, 3, 4	522

Table 2 Error matrices for unsupervised (ISODATA) and supervised (MLC) classifiers.

ISODATA classifier				
	Stressed	Healthy		**User's**
Stressed	107	74	181	0.59116
Healthy	208	156	364	0.428571
	315	230	545	
Producer's	0.339683	0.678261	**Overall**	0.482569
			Kappa	0.016636

MLC classifier					
	Stressed	Healthy	Shadow		**User's**
Stressed	225	151	5	381	0.590551
Healthy	66	74	10	150	0.493333
Shadow	24	5	206	235	0.876596
	315	230	221	766	
Producer's	0.714286	0.321739	0.932127	**Overall**	0.659269
				Kappa	0.474302

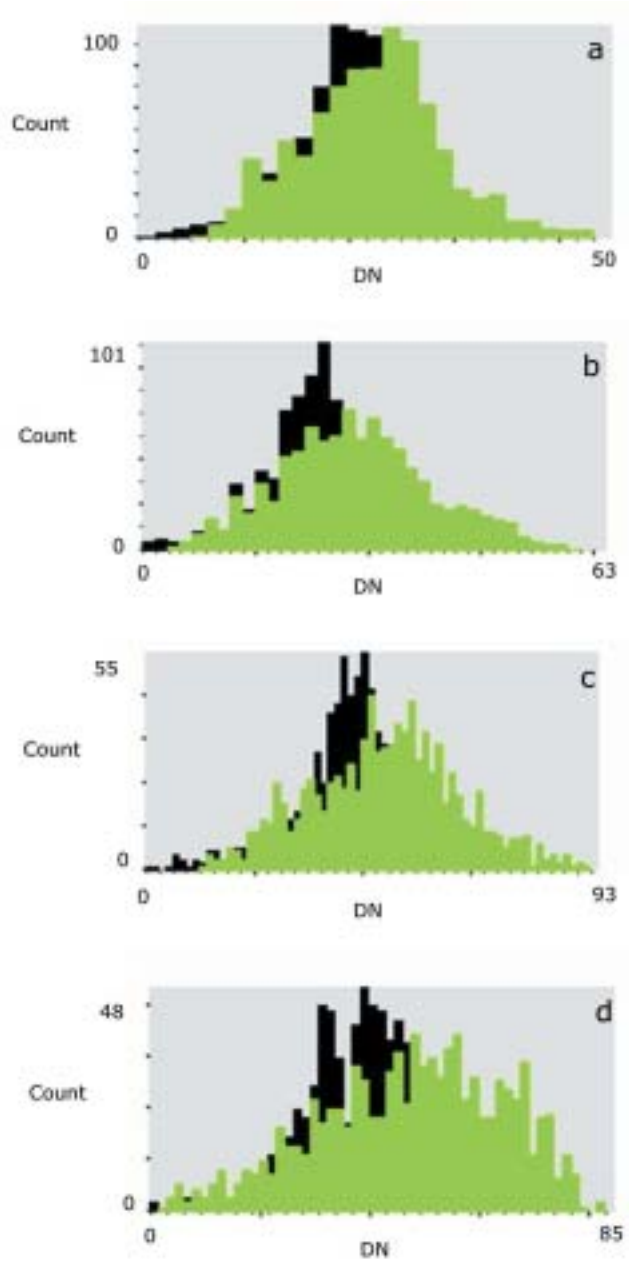

Figure 4 Histograms of digital number (DN) for training pixels.

performed poorly in separating healthy from stressed trees (overall accuracies of 48.26%), and yielded extremely high errors of omission for the stressed tree class (66% error). Khat for this method was very low: not much greater than chance. The maximum likelihood classifier produced the best overall accuracy of 65.93% and higher producer's and consumer's accuracy measures. The Kappa coefficient was also much higher (0.4743).

Discussion

The ISODATA algorithm yielded nearly 50% overall accuracy with a low K_{hat} value. Each individual tree crown classified showed dramatic striping, or spectral clustering within a tree crown. Similar results occurred when we clustered the image into more classes. The supervised maximum likelihood classifier yielded a higher accuracy than the ISODATA algorithm; however the poor transformed divergence measure indicates that separating the classes remains challenging. Indeed, the spectral histograms and the feature space ellipses tell the same story. We interpreted all these data to indicate that the spectral variances within both classes (stressed oaks and healthy oaks) within the spectral range of the ADAR sensor were larger than the variances between them, thus the ISODATA algorithm did a poor job differentiating them into two clusters. This is commensurate with what we know about the forest in this location. Healthy oaks in the area display a marked variability in canopy condition. These are 100-200 year old individuals, in an area that has a high recreation use. While *p. ramorum* is the latest disease changing the forest structure by affecting individuals, it is not the only disease in the forest. It is entirely possible that while the trees we call "healthy" show no symptoms of attack by *P. ramorum*, they are under stress for other reasons.

In addition to the fact that oaks have a variable canopy condition when healthy, these poor accuracy results can also be explained by the fact that ADAR imagery has relatively broad spectral bands that combine narrow moisture stress-sensitive regions with broader stress-insensitive regions; such combination could decrease the capability of the imagery to detect moisture stress in these forests. While some work indicates the utility of

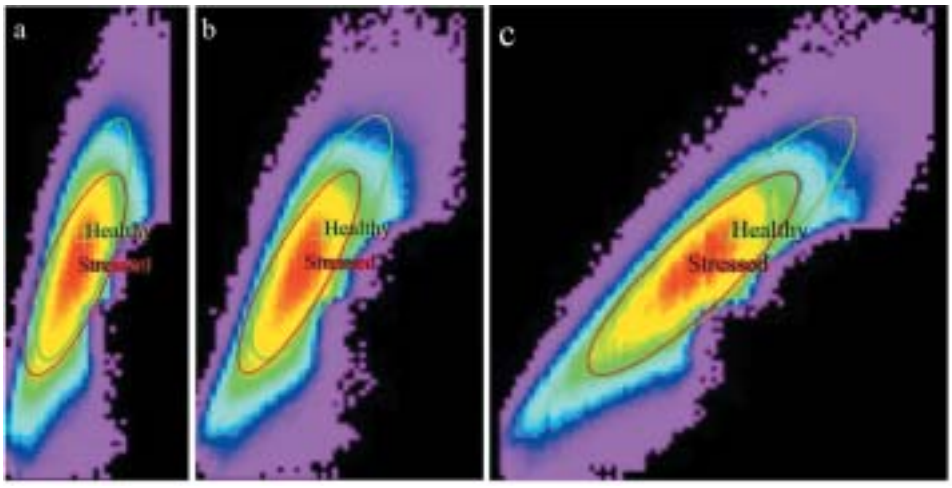

Figure 5 Feature space plots of NIR vs. bands 1-3: a) band 1, b) band 2, c) band 3 and d) band 4.

the NIR region for detecting water stress (Cibula *et al*. 1992; Gao 1996; Pu *et al*. In press; Zarco-Tejada *et al*. 2000), more studies suggest that the 1550 - 1750nm and 2080 - 2350nm region is the most favorable wavelength interval for satellite remote sensing of plant canopy water status (Ceccato *et al*. 2001; Ceccato *et al*. 2002; Downing *et al*. 1993; Gao 1996; Tucker 1980). Hyperspectral imaging should be a useful research avenue; in-situ hyperspectral data from trees in this study area has begun, and will continue (Pu *et al*. In press). Indeed, promising research using hyperspectral imaging for water moisture detection at the tree and canopy scale has been completed on several fronts (Ustin *et al*. 1998).

Timing of image acquisition is a possible additional explanatory factor. While Swiecki and Bernhardt (2002) found that moisture stress was not apparent on trees with early symptoms of the disease, nor was it a factor predisposing a tree to invasion by the pathogen, we assumed that some degree of moisture stress does precede complete canopy color change and death. We also assumed that we had sampled a cohort of trees that would likely be experiencing such stress (trees that were within one year of being completely dead, with extensive cankering and bleeding). It is possible that the moisture stress that led to the canopy change occurred much closer in time to the actual change of the canopy, and that we sampled some of these trees too early.

We said at the outset that there were scientific and management justification for this work. Here it is prudent to evaluate these results for their usefulness to a scientist mapping a cohort of stressed trees before canopy change makes them obvious, or to a forest ranger who wishes to target trees for removal or fire suppression. The best classification results yielded a Khat value of near 0.50. We interpret this result to mean that using this method one-half of the time a tree would be correctly classified as stressed. It is not entirely clear that this would assist forest managers or scientists over a large area.

Conclusions

Automated discrimination of oak trees with moisture stress from remotely sensed imagery is a challenging task, but there are obvious and pressing management justifications for attempting to do so. If the cohort of trees that are under stress for the disease could be located over broad regions from afar, proactive fire management and trails management strategies could be implemented. In addition, ecologists could better understand the landscape dynamics of the disease. However, the results of this work indicate the limitation of using ADAR imagery to map moisture stress in oaks affected with Sudden Oak Death. While the spatial resolution of the imagery is sufficient to map individual trees, the spectral resolution of the imagery, when combined with the natural variability in oak crown cover condition, makes automatic detection impossible at accuracies that are reliable for management decisions. Better accuracies can be derived (we achieved ~66% accuracy rates) using intensive field data, but it is not clear that these levels would be useful for managers or scientists. Further research into the use of hyperspectral imagery will be crucial in furthering the scientific and management goals of our project.

Acknowledgements

The research was performed under a grant from the USDA-FS and the California Department of Forestry and Fire Protection. Additional support came from the University of California Division of Agriculture and natural Resources through the Monitoring Landscape Change Workgroup.

References

Ceccato, P., Flasse, S., Tarantola, S., Jacquemoud, S. and Gregoire, J.-M., 2001. Detecting vegetation leaf water content using reflectance in the optical domain. *Remote Sensing of Environment*, 77(1): 22-33.

Ceccato, P., Gobron, N., Flasse, S., Pinty, B. and Tarantola, S., 2002. Designing a spectral index to estimate vegetation water content from remote sensing data: Part 1; Theoretical approach. *Remote Sensing of Environment*, 82(2-3): 188-197.

Cibula, W.G., Zetka, E.F. and Rickman, D.L., 1992. Response of Thematic Mapper bands to plant water stress. *International Journal of Remote Sensing*, 13(10): 1869-1880.

Cohen, W.B., 1991. Response of vegetation indices to changes in three measures of leaf water stress. *Photogrammetric Engineering and Remote Sensing*, 57(2): 195-202.

Curran, P.J., 1989. Remote sensing of foliar chemistry. *Remote Sensing of Environment*, 30: 271-278.

Downing, H.G., Carter, G.A., Holladay, K.W. and Cibula, W.G., 1993. The radiative-equivalent water thickness of leaves. *Remote Sensing of Environment*, 40: 103-107.

Duchemin, B., Guyon, D. and Lagouarde, J.P., 1999. Potential and limits of NOAA-AVHRR temporal composite data for phenology and water stress monitoring of temperate forest ecosystems. *International Journal of Remote Sensing*, 20(5): 895 - 917.

Elvidge, C.D., 1990. Visible and near infrared reflectance characteristics of dry plant materials. *International Journal of Remote Sensing*, 11(10): 1775-1795.

Erdas, 1999. Erdas Field Guide. Erdas Inc.: 1 - 672.

Everitt, J., Escobar, D., Appel, D., Riggs, W. and Davis, M., 1999. Using airborne digital imagery for detecting oak wilt disease. *Plant Disease*, 83(6): 502-505.

Flexas, J., Briantais, J., Cerovic, Z., Medrano, H. and Moya, I., 2000. Steady-state and maximum chlorophyll fluorescence responses to water stress in grapevine leaves: a new remote sensing system. *Remote Sensing of Environmen*t, 73: 283-297.

Gao, B., 1996. NDWI-A normalized difference water index for remote sensing of vegetation liquid water from space. *Remote Sensing of Environment*, 58: 257-266.

Garbelotto, M., Svihra, P. and Rizzo, D., 2001. Sudden oak death syndrome fells three oak species. *California Agriculture* (Jan/Feb 2001): 9-19.

Jensen, J., 2000. *Remote Sensing of the Environment: An Earth Resource Perspective*. Prentice Hall Series of Geographic Information Science. Prentice Hall, New Jersey, 544 pp.

Jensen, J.R., 1996. *Introductory Digital Image Processing: a Remote Sensing Perspective*, Second Edition. Prentice Hall, Upper Saddle River, NJ, 318 pp.

Kelly, M. and Meentemeyer, R.K., 2002. Landscape dynamics of the spread of Sudden Oak Death. *Photogrammetric Engineering & Remote Sensing*, 68(10): 1001-1009.

Kelly, N.M., 2002. Monitoring Sudden Oak Death in California using high-resolution imagery. USDA-Forest Service General Technical Report PSW-GTR-184: 799-810.

Kelly, N.M. and McPherson, B.A., 2001. Multi-scale approaches taken to Sudden Oak Death monitoring. *California Agriculture*, 55(1): 15-16.

Lobo, A., Marti, J.J.I. and Gimenez-Cassina, C.C., 1997. Regional scale hierarchical classification of temporal series of AVHRR vegetation index. *International Journal of Remote Sensing*, 18(15): 3167-3193.

Lyon, J.G., Yuan, D., Lunetta, R.L. and Elvidge, C.D., 1998. A change detection experiment using vegetation indices. *Photogrammetric Engineering & Remote Sensing*, 674(2): 143-150.

Macomber, S. and Woodcock, C., 1994. Mapping and monitoring conifer mortality using remote sensing in the Lake Tahoe basin. *Remote Sensing Environment*, 50: 255-266.

McPherson, B.A., Wood, D.L., Storer, A.J., Kelly, N.M. and Standiford, R.B., 2002. Sudden Oak Death: disease trends in Marin County plots after one year. USDA-Forest Service General Technical Report PSW-GTR-184: 751-763.

Pinder, J.E. and McLeod, K.W., 1999. Indications of relative drought stress in longleaf pine from Thematic Mapper data. *Photogrammetric Engineering and Remote Sensing*, 65(4): 495-501.

Pu, R., Ge, S., Kelly, N.M. and Gong, P., In press. Spectral absorption features as indicators of water status in coast live oak (Quercus agrifolia) leaves. *International Journal of Remote Sensing*.

Rizzo, D., Garbelotto, M., Davidson, J.M., Slaughter, G.W. and Koike, S.T., 2002. Phytophthora ramorum as the cause of extensive mortality of Quercus spp. and Lithocarpus densiflorus in California. *Plant Disease*, 86(3): 205-213.

Swiecki, T.J. and Bernhardt, E., 2002. Evaluation of stem water potential and other tree and stand variables as risk factors for Phytophthora canker development in coast live oak and tanoak. USDA-Forest Service General Technical Report PSW-GTR-184: 787-798.

Townsend, P.A. and Walsh, S.J., 2001. Remote sensing of forested wetlands: application of multitemporal and multispectral satellite imagery to determine plant community composition and structure in southeastern USA. *Plant Ecology*, 157: 129-149.

Tucker, C.J., 1980. Remote sensing of leaf water content in the near infrared. *Remote Sensing of Environment*, 10: 23-32.

Ustin, S.L., Roberts, D.A., Pinzon, J., Jacquemoud, S., Gardner, M., Scheer, G., Castaneda, C.M. and Palacios-Orueta, A., 1998. Estimating canopy water content of chaparral shrubs using optical methods. *Remote Sensing of Environment*, 65: 280-291.

vanAardt, J. and Wynne, R., 2001. Spectral separability among six southern tree species. *Photogrammetric Engineering and Remote Sensing*, 67(12): 1367-1376.

Zarco-Tejada, P.J., Miller, J.R., Mohammed, G.H., Noland, T.L. and Sampson, P.H., 2000. Chlorophyll fluorescence effects on vegetation apparent reflectance: II. Laboratory and airborne canopy-level measurements with hyperspectral data. *Remote Sensing of Environment*, 74: 596-608.